

## Monte Carlo Simulation of Water-Pyridine Mixtures

*André Luiz Lopes Sinoti*<sup>+a</sup>, *José Roberto dos Santos Politi*<sup>b</sup>  
and *Luiz Carlos Gomide Freitas*<sup>\*b</sup>

<sup>a</sup>*Programa de Pós-Graduação em Química, Departamento de Química,  
Universidade Federal de São Carlos, São Carlos - SP, Brazil*

<sup>b</sup>*Instituto de Química, Universidade Estadual de Campinas, C.P. 6154,  
13081-970 Campinas - SP, Brazil*

Received: September 22, 1995; Dezember 12, 1995

O método de Monte Carlo com algoritmo de Metropolis foi utilizado para calcular valores da energia média de interação e distribuições radiais de pares para a mistura binária água-piridina em função da fração molar de mistura. Os cálculos foram efetuados no ensemble isotérmico e isobárico a 298 K e 1,0 atm. Potenciais-modelo desenvolvidos para estudar os líquidos puros foram utilizados e os parâmetros necessários para calcular a energia de interação água-piridina foram obtidos com regras de cruzamento. Utilizou-se o modelo TIP4P para a água e modelos com seis e onze sítios foram utilizados para a molécula de piridina. Os cálculos foram efetuados em função da fração molar dos componentes da mistura. Valores obtidos para a energia configuracional média estão em ótimo acordo com os dados experimentais da literatura. Distribuições radiais de pares foram calculadas e mostram a formação de pontes de hidrogênio entre a água e a piridina. Distribuições radiais de pares para a interação água-água indicam a formação de aglomerados de água no interior da mistura. A contribuição da interação eletrostática para a energia de solvatação da água em diferentes meios (água pura, piridina pura e misturas equimolares água-piridina e água-metanol) foi calculada utilizando a teoria de perturbação termodinâmica. Os resultados mostram que esta contribuição, em valores absolutos, aumenta segundo a disposição piridina < água-piridina < água-metanol < água. Estes resultados mostram que a molécula de água é mais solúvel em um meio onde a tendência à formação de pontes de hidrogênio é maior, e explicam a formação de aglomerados de água no interior da mistura água-piridina. Imagens obtidas para configurações arbitrárias das misturas água-piridina e água-metanol mostram a formação de aglomerados de água na mistura com piridina e uma distribuição regular na mistura com metanol.

Thermodynamic properties and radial distribution functions for a water-pyridine mixture as a function of composition were calculated with the Monte Carlo method in the isothermal and isobaric ensemble at  $T = 298.15\text{K}$  and  $p = 1.0\text{ atm}$ . The TIP4P model was used for water and optimized potentials for liquid simulations (OPLS) force field parameters were used for pyridine. The effect of including the hydrogen atoms of pyridine was explicitly investigated by comparing the results from calculations with six and eleven site models. The results obtained for the average configurational interaction energy as a function of the mole fraction are in good agreement with experimental data. The partitioning of the total configurational energy of the water-pyridine mixture is presented and compared with similar results from other systems. Comparatively low energy values were obtained for the water-pyridine interaction. This interaction becomes slightly more negative when the hydrogen atoms of pyridine are explicitly considered. The radial distribution functions for the water-pyridine interaction show characteristic features indicating the formation of hydrogen-bonded dimers. The amplitude of the peaks observed for these distribution functions depends on the particular model used to represent the pyridine molecule. Radial distribution functions and molecular graphic representations for water-water interaction indicate the formation of small clusters of water molecules in the bulk of the water-pyridine system. This clustering enhances the water-water coordination numbers and interaction energy. The contribution from solute-solvent electrostatic

\* Present address: Departamento de Química da Universidade Federal de São Carlos, e-mail gomide@power.ufscar.br

+ Present address: Departamento de Eng. Civil - Universidade de Brasília, Brasília - DF, Brazil

interaction to the free energy of solvation of water in pure water, pure pyridine and in the equimolar water-pyridine and water-methanol mixtures were calculated using statistical perturbation theory (SPT). The results obtained for the electrostatic contribution to the free energy of solvation, in absolute values, are pyridine < water-pyridine < water-methanol < water. These free energy results indicate the migration of water molecules towards an environment rich in hydrogen bonds and explain the formation of water clusters in the bulk of water-pyridine mixtures.

**Keywords:** Monte Carlo method; liquid simulation; water-pyridine mixture

## Introduction

The investigation of the relationships between the intermolecular forces and thermodynamic properties of liquids and solutions is a fundamental subject in theoretical chemistry. Therefore, in recent years the literature shows a growing interest in the utilization of quantum chemistry and statistical mechanics methodologies to investigate these condensed phase systems<sup>1-3</sup>. Nevertheless, for most of the systems of interest, the many body nature of molecular interaction is an obstacle to the calculation of statistical mechanics averages using direct mathematical efforts. To overcome these difficulties, computer simulation methodologies such as Monte Carlo (MC) and molecular dynamics (MD) have been largely used to obtain average values of thermodynamic functions. Using MC and MD calculations, thermodynamic properties of pure liquids and solute-solvent systems have been investigated<sup>3-9</sup>. In contrast to the advances achieved in the theoretical investigations of pure liquids, comparatively few results have been reported for binary mixtures.

In recent years in our laboratory we have undertaken a theoretical investigation of binary liquid mixtures, with a special emphasis on the relationships between hydrogen bonding and thermodynamic properties<sup>10,11</sup>. The present paper includes Monte Carlo results for the water-pyridine system as a function of concentration. The energies of interaction, radial distribution functions and coordination numbers were calculated and compared with experimental data and the results obtained from other systems. The results for water-water interaction show the formation of water clusters in the bulk of the water-pyridine system. Our results led to the proposal that the formation of water clusters in the bulk of some water-organic liquid mixtures can be explained by general rules of equilibrium dislocation<sup>12</sup>. In such an interpretation, the enhancement of the water-water interaction is induced by weak interactions between water and the organic liquid. To further investigate this topic, the contributions from electrostatic forces to the free energy of solvation of water molecules in different solvents were calculated using statistical perturbation theory (SPT)<sup>13</sup>. In absolute values, our results show a decrease on the free energy of solvation of water as the concentration

of the organic liquid is increased. This behavior of the free energy of solvation can be associated with a decrease in the number of hydrogen bond interactions between the solute (water) and solvent molecules. Therefore, numerical modifications in the population of hydrogen bonded dimers in these systems, as a function of the mole fraction, leads to differences in water organization. As has been shown by different experimental methods, physico-chemical properties of aqueous solutions of some organic liquids exhibit anomalous behavior as a function of concentration<sup>14-16</sup>. The results presented in this paper emphasize the importance of studying water organization in these solutions as a significant step towards understanding the physico-chemical behavior of these systems.

## Methodology

### The intermolecular potential function

In this study all the molecules were represented by rigid structures and the polarization effects were neglected. The interaction energy,  $E_{ab}$ , between molecules **a** and **b** was calculated by adding the contributions from Lennard-Jones and Coulomb potentials centered in molecular sites, that is

$$E_{ab} = \sum_i^{\text{on a}} \sum_j^{\text{on b}} \left[ \frac{A_{ij}}{r_{ij}^{12}} - \frac{B_{ij}}{r_{ij}^6} + \frac{q_i q_j}{r_{ij}} \right] \quad (1)$$

In this equation  $r_{ij}$  is the distance between site  $i$  in **a** and site  $j$  in **b**. The parameters  $A_{kk}$  and  $B_{kk}$  for a given site  $k$  were defined by  $A_{kk} = 4\epsilon_k \sigma_k^{12}$  and  $B_{kk} = 4\epsilon_k \sigma_k^6$ . In these expressions  $\epsilon_k$  and  $\sigma_k$  are the Lennard-Jones parameters for the  $k^{\text{th}}$  molecular site. Parameters  $A_{ij}$  and  $B_{ij}$  for a non-diagonal interaction  $[ij]$  were obtained using geometric combining rules<sup>3</sup>,  $A_{ij} = (A_{ii} A_{jj})^{1/2}$  and  $B_{ij} = (B_{ii} B_{jj})^{1/2}$ . The parameters used in this study were taken from the TIP4P model for representing water molecules, and the optimized potentials for liquid simulations (OPLS) force field was used for pyridine<sup>17-20</sup>. As discussed by Jorgensen *et al.*<sup>17-20</sup>, the OPLS partial charges  $\{q_i, q_j\}$  are distributed along the molecular geometry and optimized to represent the contribution from charge density asymmetry to the intermolecular interaction energy. As a general trend, the dipole moment produced by a given partial charge distribution in the OPLS force field is overestimated by *ca.* 10-20% to

compensate for the neglect of the polarization effects. Two OPLS models were used to represent pyridine molecules:

a) a six site model, in which<sup>18</sup> each CH group of pyridine is considered as an united atom site, and

b) an eleven site model<sup>19</sup> with the explicit inclusion of all hydrogen atoms. The partial charges used in this model were calculated with 6-31G\* basic functions using the CHELPG procedure included in the Gaussian 92 program<sup>21</sup>.

The parameters  $A_{ij}$  and  $B_{ij}$  needed to calculate the water-pyridine interaction were obtained using the potential functions for the pure liquids and the combining rules presented above. No further attempt was made to optimize them. This procedure is justified, since the results reported for the free energy of hydration of pyridine, using the same potential models and combining rules, are in excellent agreement with experimental data<sup>19</sup>.

#### Monte Carlo simulations

Statistical mechanics simulations were carried out in the isothermal and isobaric ensemble at  $T = 298.15$  K and  $p = 1.0$  atm using the Monte Carlo method. Standard procedures were used, including Metropolis importance sampling<sup>22</sup> and cubic box boundary conditions<sup>2,3</sup>. The FORTRAN code DIADORIM, developed by one of us was used<sup>23</sup>. The simulations of the binary liquid mixtures were carried out with an overall number of 256 molecules in the reference box. In the calculation of binary mixtures, the number of water and organic molecules were appropriately chosen to reproduce the mole fraction. The initial volume of each simulation box was calculated using the experimental densities of the pure liquids, and also considering an ideal mixing process. The initial coordinates of the molecules in the simulation box were obtained by replacing randomly chosen organic molecules from a previously equilibrated box with TIP4P water.

New configurations were generated by randomly translating and rotating a randomly chosen molecule. Ranges for translations and rotations were adjusted to yield an acceptance/trial ratio of about *ca.* 0.45 for new configurations. As in the isothermic and isobaric ensemble the volume is not fixed new configurations were also generated by volume changes. After a volume change, the center of mass coordinates of all molecules in the reference box were scaled in the usual way described in the literature<sup>2,3</sup>. The maximum range for a volume change was adjusted to yield the same acceptance/trial ratio as the above. A volume change was tried every 1000 configurations. To calculate the configurational energy, a full intermolecular interaction was considered whenever the site-to-site distance  $r_{ij}$  in Eq. 1 fell below the cut-off radius  $r_c = 10.0$  Å. The contribution of the Lennard-Jones potential beyond the cut-off radius was included using the formalism presented by Allen and Tildesley<sup>3</sup>.

The need to include long range correction of the Coulombic potentials was also investigated. As a general trend, the long range correction calculated using the Ewald sum formalism<sup>3</sup> was found to be negligible for the systems under consideration in the present work. This small contribution of long range correction to the Coulombic attraction is due to the fact that the species studied here are neutral. The studies of size dependence on similar systems also indicate that this long range contribution can be safely neglected<sup>10,11</sup>. In each simulation an equilibration step with  $1 \times 10^6$  configurations was done and the average phase was accomplished with  $5 \times 10^6$  new configurations. Statistical uncertainties were calculated from separate averages in blocks of  $1.0 \times 10^5$  configurations.

#### Free energy calculations

Statistical perturbation theory (SPT) has been established as a valuable methodology for calculating free energy<sup>13,24-26</sup>. Using the SPT formalism, the free energy difference  $[G_B - G_A]$  between two states A and B whose Hamiltonians are, respectively,  $H_A$  and  $H_B$ , is given by,

$$\Delta G = G_B - G_A = -k_B T \ln \langle - (H_B - H_A) / k_B T \rangle_A \quad (2)$$

In this equation  $k_B$  is the Boltzmann constant and  $T$  is the temperature.

Equation 2 gives the free energy difference as an average of the energy difference between states A and B. This average is evaluated by a sampling based on system A. When systems A and B are too different, the convergence of the averaging in Eq. 2 may be slow<sup>13</sup>. To overcome this problem, the simulation is divided into parts by using a coupling parameter,  $\lambda$ , which is then used to represent the adiabatic transformation of system A into B. For a transformation of A into B the intermediate values of a given feature of the system, generically represented by  $\Xi$ , are defined by,

$$\Xi(\lambda) = \lambda \Xi_B + (1 - \lambda) \Xi_A \quad (3)$$

When the parameter  $\lambda$  goes from 0 to 1, the intermediate values  $\Xi(\lambda)$  change from  $\Xi_A$  to  $\Xi_B$ . As discussed in the literature, the SPT methodology is very useful for calculating the free energy of solvation and good agreement with experimental results has been reported<sup>13,19, 25-27</sup>.

In this work the statistical perturbation theory was used to calculate the contribution of solute-solvent electrostatic interaction to the free energy of solvation of TIP4P water in pure water, pure pyridine and in equimolar water-pyridine and water-methanol mixtures. As discussed below, this calculation was performed with the annihilation of the partial charges of TIP4P water using Eq. 2. The result obtained in this step is the full contribution of solute-solvent electrostatic interaction to the free energy of solvation. In the OPLS force field the hydrogen bonding is given by

the coulombic interaction between the acidic hydrogen and an electronegative site. Therefore, the free energy result obtained in this step is an upper limit to hydrogen bonding contributions to the free energy of solvation of TIP4P water in the solvent being considered. The procedure outlined above is similar to the one used by Jorgensen *et al.*<sup>27</sup> to calculate the free energy of hydration of TIP4P water. As specified above, for each interval needed in the mutation of water, an equilibration step with  $1 \times 10^6$  configurations was carried out and the average phase was accomplished with  $5 \times 10^6$  new configurations. Preferential sampling was used to choose the appropriate solvent molecules to attempt the Monte Carlo moves<sup>28</sup>. With this procedure the solvent molecules nearest to the solute were moved *ca.* twice as often compared to molecules in the bulk solution. The statistics for acceptance/rejection of trial movements for solute and solvent molecules followed the same constraint discussed above for the calculation of binary mixtures. To be consistent with the earlier calculation of the free energy of hydration of TIP4P water<sup>27</sup>, a cutoff of 8.5 Å was used for solute-solvent interaction. To account for convergence procedures, the solute-solvent interaction energy was multiplied by a switching function<sup>29</sup> in the interval [8.0-8.5 Å]. With this switching function the solute-solvent interaction energy is smoothly reduced to zero on the boundary of the sphere defined by the cut-off length. The computational cost of the calculation was shortened by using the double wide-sampling procedure<sup>13,25</sup>. All calculations were carried out on IBM RISC 6000 and HP Apollo 720 workstations.

## Results and Discussions

### Energetics and radial distribution functions

The present Monte Carlo results for the average configurational energy as a function of the water mole fraction were compared with experimental data in Table 1. As discussed in the footnote below Table 1, the experimental data for the configurational energy were derived from experimental results for the energy of mixing as a function of concentration and heat of vaporization for pure liquids. In an overall appreciation, the difference between the theoretical and experimental results in Table 1 is approximately 0.50 kcal/mol. Considering the many body nature of the system under investigation, this agreement can be considered very good. Comparing results from the two different OPLS models used for pyridine, the energies calculated with the eleven site model are systematically more negative. We present in Fig. 1 a partitioning of the water-pyridine interaction energy as a function of the mole fraction, showing the contribution of each type of interaction to the total energy. The data in Fig. 1 were calculated using the OPLS six site model for pyridine. As already defined in Eq. 1, it is worth noting that this energy partitioning is a

**Table 1.** Average configurational energy  $E_i$  (kcal/mol), for the water-pyridine mixture as a function of water mole fraction  $X_w$ .

water mole fraction, $X_w$	$E_i$ , present research <sup>a</sup>	$E_i$ , experimental <sup>b</sup>
0.000	-9.05 ± 0.02	-9.12
0.125	-8.67 ± 0.02	-9.04
0.250	-8.76 ± 0.01 [-9.43 ± 0.02]	-9.03
0.375	-8.87 ± 0.02	-9.07
0.500	-8.97 ± 0.02 [-9.63 ± 0.03]	-9.16
0.625	-9.03 ± 0.02	-9.31
0.750	-9.26 ± 0.02 [-9.77 ± 0.01]	-9.50
0.875	-9.64 ± 0.02	-9.71
1.000	-10.18 ± 0.02	-9.00

a- The results in [ ] were calculated using the eleven site model for pyridine. All the others were obtained with the six site model.

b- The values of  $E_i$  (experimental) were obtained from the relationships:

$$1) \Delta H_{\text{vap},k} = -E_{i,k} + RT, \text{ and}$$

$$2) \Delta H_{\text{vap},\text{mix}} = H^E + [X_w \Delta H_{\text{vap},w} + (1-X_w) \Delta H_{\text{vap},py}]$$

where  $\Delta H_{\text{vap},k}$  is the enthalpy of vaporization of liquid k,  $E_{i,k}$  is the average configurational energy of liquid k,  $RT = 0.593$  kcal/mol at  $T = 298\text{K}$ ,  $H^E$  is the excess enthalpy of mixing, and  $X_w$  the mole fraction of water. Experimental results for excess energies are from Refs. 37 and 38 and the heat of vaporization of water and pyridine are from Refs. 39 and 40.

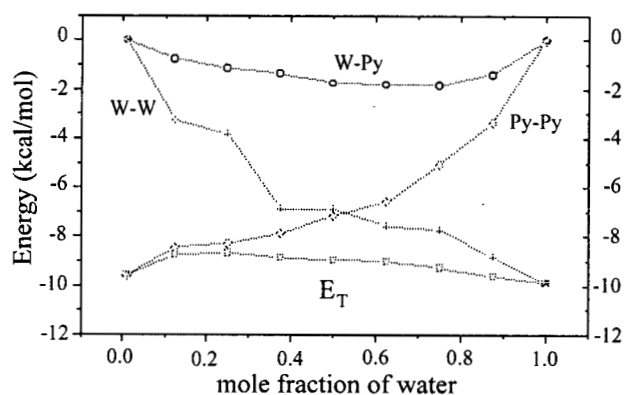


**Figure 1.** Partitioning of the total energy (kcal/mol) for the water-pyridine mixture as a function of the water mole fraction.

Captions: W-W: Energy from water-water interaction; W-Py: Energy from water-pyridine interaction; Py-Py: Energy from pyridine-pyridine interaction;  $E_T$ : Total configurational energy.

consequence of the pair additive approximation used for the potential interaction. The behavior of the interaction energies as a function of the mole fraction follows the general pattern expected for a binary mixture: the contribution from each component increases as its concentration is raised. As a general trend, the contribution from the water-pyridine interaction to the total energy is small. It is inter-

esting to compare the present results with similar information from other binary mixtures previously studied in our laboratory. In Table 2, energy partitioning results from some equimolar mixtures are compared to the present ones for the water-pyridine system. Comparatively, the data in Table 2 show a general tendency towards enhancement in water-water interaction energy as the water-liquid 2 interaction energy decreases. Considering the change in water-liquid 2 interaction a perturbation, this behavior can be understood as a consequence of rules for equilibrium dislocation<sup>12</sup> in dynamic systems: the enhancement observed for water-water interaction is a compensating change due to the decrease in the water-liquid 2 interaction energy. To understand this behavior on a molecular basis, it is interesting to associate the energetics of these binary mixtures with correlation functions.

In Fig. 2 radial distribution functions (RDF) for water-pyridine interaction at two concentrations are shown. The results from calculations with six and eleven site models for pyridine are shown. For both models are clear on the H-N RDF (curves labeled a in Fig. 2) the features normally found for hydrogen-bonded liquids<sup>10,11,17,20,30</sup>. The position of the peak on these curves,  $r \approx 2.0 \text{ \AA}$ , is not far from the hydrogen-nitrogen distance ( $d(\text{H-N}) = 1.85 \text{ \AA}$ ) calculated for a water-pyridine dimer in gas phase with molecular mechanics<sup>31</sup>. The peaks near  $r \approx 3.0 \text{ \AA}$  in the oxygen-nitrogen correlation (curves labeled b in Fig. 2) are also associated with hydrogen-bonded dimers. In the present work, radial distribution functions for water-pyridine interactions were calculated as a function of the water mole fraction. An overall analysis of these results shows a negligible dependence of the radial positions of the features attributed to hydrogen-bonding with the water mole fraction. The influence of the potential model used for the pyridine molecule on the position of these peaks is also small. However, as can be observed in Fig. 2, the amplitudes of these peaks are strongly dependent on the potential

model used to represent the pyridine molecule. This dependence can be associated with the value of the partial charge over the nitrogen site. In the eleven site model this charge is  $q(\text{N}) = -0.679e$ , compared with  $q(\text{N}) = -0.490e$  used in the six site OPLS model. Therefore, the more negative value for the partial charge over the nitrogen atom in the eleven site model leads to an increase in hydrogen bonding and to a higher amplitude in the H-N and O-N RDF. Furthermore, the enhancement observed in the RDF when the eleven site model is used explains the more negative values obtained for the water-pyridine interaction energy, as already shown in Table 1.

Peaks on RDF can be associated with solvation shells. As discussed elsewhere, the coordination number for a given site-site interaction is proportional to the integral of the RDF over the first maximum to the position of the first minimum<sup>3</sup>. Coordination numbers obtained for water-water interaction in some binary mixtures are presented in Table 3. For completeness, coordination numbers for pure

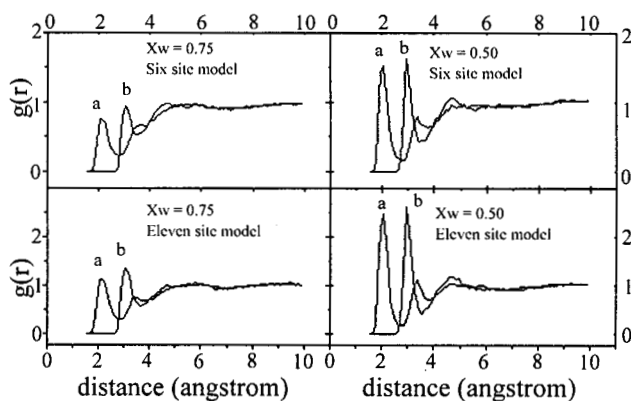


**Figure 2.** Radial distribution functions for water-pyridine interaction at water mole fraction  $X_w = 0.50$  and  $X_w = 0.75$ . Calculations performed using six and eleven site models for pyridine.

Captions: a = Hydrogen-nitrogen site-site correlation; b = Oxygen-nitrogen site-site correlation.

**Table 2.** Partitioning of the average configurational energy for some equimolar mixtures. Energies for pure liquids are also included.

system	$EL_{11} / n_1$	$EL_{22} / n_2$	$E(L_{12}) / (n_1+n_2)$	$E(\text{total}) / (n_1+n_2)$
pure water	-10.18	-	-	$-10.18 \pm 0.02$
pure pyridine (6s)	-9.05	-	-	$-9.05 \pm 0.03$
water-THF*	-7.45	-6.00	-1.95	$-8.68 \pm 0.02$
water-pyridine (6s)	-6.28	-7.01	-2.07	$-8.97 \pm 0.02$
water-pyridine (11s)	-5.87	-7.29	-3.05	$-9.63 \pm 0.03$
water-methanol **	-5.43	-4.58	-4.46	$-9.56 \pm 0.02$

$EL_{ij}/n_i$  = Total ( $L_i - L_j$ ) interaction energy / number of interacting molecules.

$L_1$  = first liquid in column 1;  $L_2$  = second liquid in column 1.

6s = six site model for pyridine, Ref. 18.

11s = eleven sites model for pyridine, Ref. 19.

\* water-THF (tetrahydrofuran) Ref. 11.

\*\* water-methanol, Ref. 10.

water are also presented. The coordination numbers for the water-water interaction in the water-pyridine mixture, calculated using both pyridine models, are very close, but the ones from the TIP4P-pyridine six site model calculation are slightly greater. Very interesting correlations between the results shown in Table 2 and Table 3 are achieved if a decrease in the water-liquid 2 interaction is associated with an increase in the water-water coordination number. This increase in the coordination numbers can also be associated with more negative values for the water-water interaction energy. Therefore, as presented above, the enhancement of the water-water interaction can be associated with a weak interaction between water and the organic liquid. A comparison of the water-water coordination numbers in Table 3 indicates that the pyridine and THF liquids make water clusters. This effect can be further analyzed using computer graphics facilities.

The search for relationships between thermodynamic behavior and molecular organization is one powerful application of molecular modeling through computer simulations. In Fig. 3, we present distributions of water molecules extracted from equimolar water-pyridine and water-methanol mixtures<sup>32</sup>. These configurations were taken at random from simulation boxes containing 200 TIP4P water and 200 molecules of the corresponding organic liquid. In these figures only the water molecules are shown. The molecular distributions in Fig. 3a show the clustering of water molecules in the bulk of the water-pyridine mixture. The formation of these water clusters is almost independent of the particular type of model potential used to represent the pyridine molecule. Therefore, the formation of these clusters explains the enhancement of the water-water interaction energy shown in Table 2. Theoretical results indicating the clustering of water molecules were reported in an earlier study of water-tetrahydrofuran (THF) mixtures<sup>11</sup>. Glew and Watts<sup>33</sup>, in their paper discussing the energetics of water-THF mixtures, proposed that oxygen sites of THF

molecules mainly interact with non-hydrogen-bonded OH groups present in the bulk of water. The results for water-water and water-pyridine interactions in the present work allows for the same interpretation, that is, the nitrogen sites of pyridine molecules mainly interact with non-hydrogen-bonded hydrogen sites of water.

Contrasting with the water configuration shown in Fig. 3a, it is interesting to observe the uniform distribution of water molecules in the water-methanol mixture in Fig. 3b. In this mixture an intercalation between water and methanol molecules is observed. This intercalation explains the average number of hydrogen bonds between water and methanol molecules (1.41), that is, each water molecule is interacting with more than one methanol molecule. This number is to be compared with the value 0.55-0.77, the average number of hydrogen bonds found between water and pyridine molecules. This spatial arrangement of water and methanol molecules is in agreement with interaction energies, Table 2, and coordination numbers, Table 3, obtained for water-methanol mixtures.

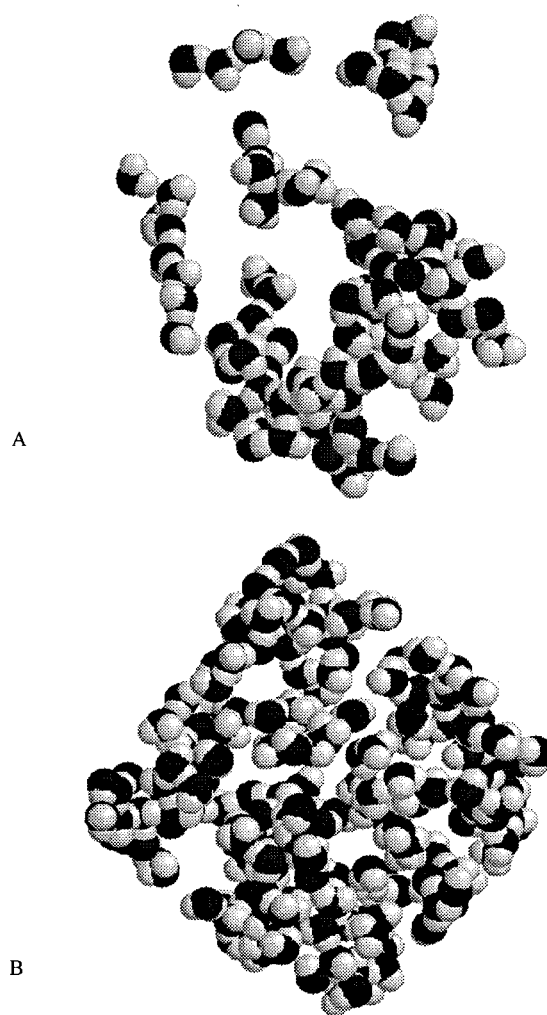


**Table 3.** Coordination numbers (CN) for water-water interaction in pure water and some water-organic liquid equimolar mixtures.

System\CN	O-O	H-O
TIP4P (pure water)	4.95	3.95
TIP4P-THF	3.58	2.89
TIP4P-py(6s)	2.92	2.50
TIP4P-py(11s)	2.59	2.27
TIP4P-methanol	2.44	2.12

O-O - average oxygen site-site coordination number.

H-O - average number of hydrogen bonds per molecule.

Py(6s) - six site model for pyridine molecule.

Py(11) - eleven site model for pyridine molecule.

TIP4P - methanol data from Ref. 10.

TIP4P - THF (tetrahydrofuran) data from Ref. 11.

**Figure 3.** Spatial distribution of water molecules in water-pyridine (a) and water-methanol (b) equimolar mixtures.

The organization of water molecules induced by an apolar solute site is generally presented as the hydrophobic effect<sup>34</sup>. As extensively discussed in the literature<sup>35</sup>, the rearrangement of water has very important consequences for the interplay between solvation thermodynamics and the conformational stability of many biological molecules. To further investigate the dependence of the clustering process on the potential model used for pyridine, in Fig. 4 we present the RDF for water-water interaction in water-pyridine mixtures obtained with the model used to represent pyridine. The position of the peaks on the H-O ( $r \approx 1.85 \text{ \AA}$ ) and O-O ( $r \approx 2.76 \text{ \AA}$ ) correlation curves are almost the same in both calculations. The peaks calculated using the six site model for pyridine are slightly higher than the ones obtained with the eleven site model. These differences lead to a small increase in the water-water coordination number when the six site model is used and, as already shown in Table 2, to a more negative value for the water-water interaction energy. The investigation of the effects of including hydrogen sites of solutes in solvation studies<sup>19,36</sup> is of great importance for the improvement of molecular models and computational cost. As an overview of the present results, the inclusion of hydrogen sites in the pyridine model leads to small but detectable influences on the interaction energy and spatial organization of water molecules.

#### Free energy of solvation of TIP4P water in pyridine and water-pyridine mixture

In this section the partial contributions from electrostatic interaction to the free energy of solvation of TIP4P water in pure pyridine, pure water and equimolar water-pyridine and water-methanol mixtures are presented. The calculations were performed with the SPT formalism following the methodology discussed above. To overcome some numerical instabilities, the mutation of TIP4P water was performed through small variations,  $\Delta\lambda = 0.1$ , on the

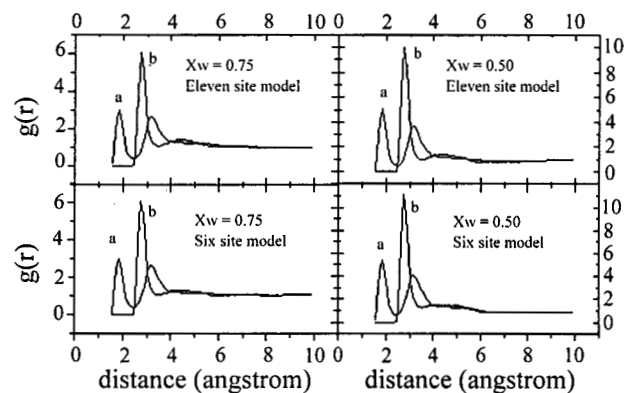


**Figure 4.** Radial distribution functions for water-water interaction in water-pyridine mixtures at water mole fraction  $X_w = 0.50$  and  $X_w = 0.75$ . Calculations performed using six and eleven site models for pyridine. Captions: a = Hydrogen-oxygen site-site correlation; b = Oxygen-oxygen site-site correlation.

coupling parameter  $\lambda$ , a procedure similar to the one used by Jorgensen *et al.*<sup>27</sup>. The mutation of water to a chargeless site is an adequate procedure to switch off all the electrostatic interactions between solute and solvent molecules. It is worth noting that hydrogen bonding in the OPLS force field is represented by coulombic attraction between the acidic hydrogen and, in the present case, the oxygen and nitrogen sites. Therefore, the free energy calculated along this mutation path gives the overall contribution from hydrogen bonding, dipole-dipole interactions, etc., to the free energy of solvation. To avoid lengthy simulations, the double-wide sampling procedure<sup>13</sup> was used throughout the free energy calculation. The results obtained as a function of the coupling parameter  $\lambda$  in the four solvents listed above are shown in Fig. 5. The free energy results increase in the sequence pyridine < water-pyridine < water-methanol < water. Therefore, the formation of water clusters in the bulk of water-pyridine mixtures can be explained by a spontaneous migration of water molecules to a water-rich environment. In the clustering process, the overall electrostatic binding energy of water to its surroundings is increased, leading to a decrease on the free energy of the system. In Fig. 5 it is interesting to note the difference in the free energy necessary to convert water to a chargeless

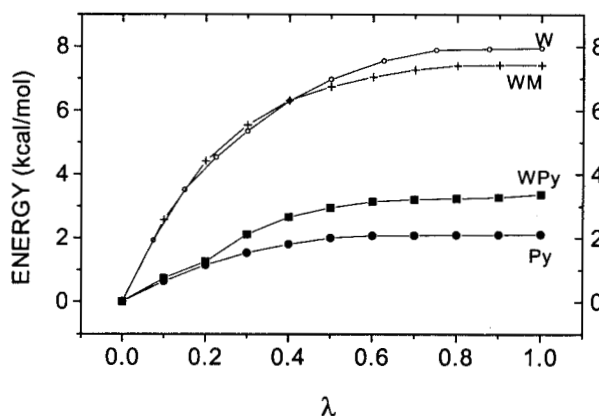


**Figure 5.** Contribution of the electrostatic solute(water)-solvent interaction to the free energy of solvation (absolute value) as a function of the coupling parameter  $\lambda$ . Calculation performed at  $T = 298\text{K}$  and  $p = 1.0 \text{ atm}$ . Captions: W - solvation of water in pure water; WM - solvation of water in the equimolar water-methanol mixture; WPy - solvation of water in the equimolar water-pyridine mixture; Py - solvation of water in pure pyridine.

**Table 4.** Coordination numbers (CN) from equimolar mixtures of pyridine with water.

System\CN	O-N	H-N
TIP4P-py(6s)	0.62	0.55
TIP4P-py(11s)	0.86	0.77

O-N - interaction of oxygen with nitrogen from pyridine.

H-N - interaction of hydrogen sites with nitrogen from pyridine.

site in pure water and in an equimolar water-methanol mixture, which is only 0.6 kcal/mol. This small difference can be attributed to the fact that the number of hydrogen bonds between solute (water) and solvent molecules are close for both systems: the integration of the hydrogen-oxygen solute-solvent RDF gives 3.95 and 3.50, respectively, for the number of hydrogen bonds between solute and solvent molecules in pure water and in the equimolar water-methanol mixture<sup>10</sup>. As a consequence of this similarity in the free energy of solvation, there is a small tendency towards the formation of water clusters in water-methanol mixtures. This result agrees with the uniform distribution of water molecules shown on Fig. 3b.

## Conclusions

Results for water-pyridine mixtures calculated with the Monte Carlo method in the isothermic and isobaric ensemble were presented. Values obtained for the average configurational energy as a function of concentration is in good agreement with experimental data. These results verify the quality of the potential functions used in this work and the usefulness of combining rules to obtain parameters for cross interactions. The total configurational energy of the water-pyridine mixture was partitioned and compared with similar results from water-methanol and water-tetrahydrofuran (THF) mixtures. This comparison shows an enhancement of water-water coordination numbers and interaction energy as the water-organic liquid interaction energy decreases. This increase in water-water interaction can be explained by an equilibrium dislocation towards a overall stabilization of the system. Molecular graphics for the spatial distributions of water molecules in water-methanol and water-pyridine equimolar mixtures were presented. These graphics show a homogeneous distribution of water molecules in water-methanol and the formation of water clusters in the water-pyridine mixture. This effect was further investigated by the calculation of the contribution of electrostatic interaction to the free energy of solvation of TIP4P water in pure pyridine, water-pyridine and water-methanol mixtures. In absolute values, the results show a free energy increase in the sequence pyridine < water-pyridine < water-methanol < water. Therefore, the stability increases as the water molecule moves towards an environment rich in hydrogen bonds. These free energy results explain the formation of water clusters in water-pyridine mixtures and the homogeneous distribution of water molecules in the water-methanol mixture.

## Acknowledgments

The authors wish to thank FAPESP (Fundação de Amparo a Pesquisa do Estado de São Paulo) and CNPq (Conselho Nacional de Desenvolvimento Científico e Tecnológico) for support for this research. JRSP and ALLS

also thank CNPq for scholarships. The authors are grateful to CENAPAD-SP for providing computational facilities.

## References

1. Hansen, J.P.; McDonald, I.R.; *Theory of Simple Liquids*; Academic Press; London, 1986.
2. Hermann, D.W.; *Computer Simulation Methods*; Springer-Verlag; Berlin, 1986.
3. Allen, M.P.; Tildesley, D.J.; *Computer Simulation of Liquids*; Oxford Press; Oxford, 1987.
4. Kovacs, H.; Kowalewski, J.; Laaksonen, A.; *J. Phys. Chem.* **1990**, *94*, 7378.
5. Pálinkás, G.; Bakó, I.; *Z. Naturforsch. Teil A* **1991**, *46*, 95.
6. Jorgensen, W.L.; *Chemtracts-Organic Chemistry* **1991**, *4*, 91.
7. Straatsma, T.P.; MacCammon, J.A.; *Annu. Rev. Phys. Chem.* **1992**, *43*, 407.
8. Teixeira-Dias, J.J.C.; *Molecular Liquids: New Perspectives in Physics and Chemistry*; Kluwver Acad. Pub., NATO ASI series, 1992.
9. Arêas, E.P.G.; Pascutti, P.G.; Schereier, S.; Munding, K.C.; Bisch, P.M.; *J. Phys. Chem.* **1995**, *99*, 14885.
10. Gomide Freitas, L.C.; *J. Mol. Struct.(THEOCHEM)* **1993**, *282*, 15.
11. Gomide Freitas, L.C.; Cordeiro, J.M.M.; *J. Mol. Struct. (THEOCHEM)* **1995**, *335*, 189.
12. De Heer, J.; *Phenomenological Thermodynamics*; Prentice-Hall; Englewood Cliffs, NJ, 1986.
13. Van Gunsteren, W.F.; Weiner, P.K.; Ed.; *Computer Simulations of Biomolecular Systems*; ESCOM, Leiden, 1989.
14. Cser, L.; Jancsó, G.; Papoular, R.; Grósz, T.; *Physica B* **1989**, *156-157*, 145.
15. Santos, P.S.; Arêas, E.P.G.; personal communication.
16. Mezei, M.; Jancsó, G.; *Chem. Phys. Lett.* **1995**, *239*, 237.
17. Jorgensen, W.L.; Chandrasekar, J.; Madura, J.D.; Impey, R.W.; Klein, M.L.; *J. Chem. Phys.* **1983**, *79*, 926.
18. Jorgensen, W.L.; Briggs, J.M.; Contreras, M.L.; *J. Phys. Chem.* **1990**, *94*, 1683.
19. Carlson, H.A.; Nguyen, T.B.; Orozco, M.; Jorgensen, W.L.; *J. Comp. Chem.* **1995**, *14(10)*, 1240.
20. Jorgensen, W.L.; *J. Chem. Phys.*, **1986**, *90*, 1276.
21. Frisch, M.J.; Trucks, G.W.; Head-Gordon, M.; Gill, P.M.W.; Wong, M.W.; Foresman, J.B.; Johnson, B.G.; Schlegel, H.B.; Robb, M.A.; Replogle, E.S.; Gomperts, R.; Andres, J.L.; Raghavachari, K.; Binkley, J.S.; Gonzales, C.; Martin, R.L.; Fox, D.J.; Defrees, D.J.; Baker, J.; Stewart, J.J.P.; Pople, J.A.; *Gaussian 92*; Gaussian, Inc.; Pittsburgh, PA, 1992; revision A.



22. Metropolis, N.; Rosebluth, A.W.; Rosebluth, M.N.; Teller, A.H.; Teller, E.; *J. Chem. Phys.* **1953**, *21*, 1087.
23. Gomide Freitas, L.C.; Program DIADORIM (FORTRAN code); Departamento de Química, UFSCar, 1992.
24. Zwanzig, R.W.; *J. Chem. Phys.* **1954**, *22*, 1420.
25. Mezei, M.; Beveridge, D.L.; *Ann. N. Y. Acad. Sci.*, **482**, 1 (1986).
26. Pearlman, D.A.; *J. Phys. Chem.* **1994**, *98*, 1487.
27. Jorgensen, W.L.; Blake, J.F.; Buckner, J.K.; *Chem. Phys. Lett.* **1989**, *129*, 193.
28. Owicki, J.C.; *ACS Symp. Ser.* **1978**, *86*, 159.
29. Andrea, T.A.; Swope, W.C.; Andersen, H.C.; *J. Chem. Phys.* **1983**, *79*, 4576.
30. Landanyi, B.M.; Skaff, M.S.; *Annu. Rev. Phys. Chem.* **1993**, *44*, 335.
31. *PCModel*, Serena Software, Bloomington, USA.
32. Rasmol Program, v. 5, developed by Roger Sayle, Biomolecular Structure Group & Development, UK, 1994.
33. Glew, D.N.; Watts, H.; *Can. J. Chem.* **1973**, *51*, 1933.
34. Ben-Naim, A.; *Hydrophobic Interactions*; Plenum Press; New York, 1985.
35. Vasquez, M.; Némethy, G.; Scheraga, H.A.; *Chem. Rev.* **1994**, *94*, 2183.
36. Kaminski, G.; Duffy, E.M.; Matsui, T.; Jorgensen, W.L.; *J. Chem. Phys.* **1994**, *98*, 13077.
37. Wóycicka, M.; Kurtika, Z.; *Bull. Acad. Sci. Pol. Sci. Ser. Sci. Chim.* **1965**, *13*, 469.
38. Christensen, J.J.; Hanks, R.W.; Izatt, R.M.; *Handbook of Heats of Mixing*; Wiley; New York, 1982.
39. Riddick, J.A.; Bunger, W.B.; *Organic Solvents*; Wiley-Interscience; New York, 1970.
40. Marcus, Y.; *Ion Solvation*, Wiley, New York, 1985.

FAPESP helped in meeting the publication costs of this article